

Chapter 2

Theory and Formalism

Elastic (quasi-elastic) scattering from a proton (nucleon) can be described to first order as a single photon (γ) exchange for the electromagnetic interaction and single vector boson (Z) exchange for the neutral weak interaction, as shown in the Feynman diagrams in Fig. 2.1.

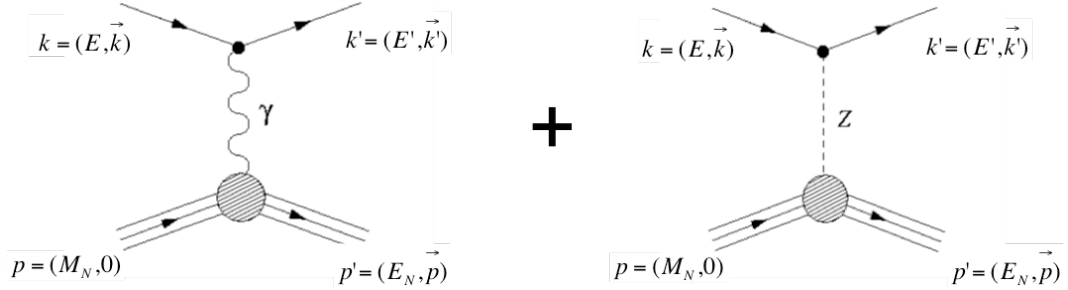


Figure 2.1: *Total leading order amplitude for electron scattering from a nucleon is the sum of the leading order electromagnetic and neutral current amplitudes.*

The incident electron, e , described by the four-vector $k = (E, \vec{k})$ scatters from a target nucleon, $p = (M_N, 0)$. After the scattering event, the electron is described as $k' = (E', \vec{k}')$ and the nucleon as $p' = (E_N, \vec{p}')$. The four vector representing the energy and momentum lost by the electron is $Q = (\omega, \vec{q})$ where $\omega = E - E'$ and $\vec{q} = \vec{k} - \vec{k}'$. The electron is treated in the extreme relativistic limit, so that $m_e^2 = 0$. Q^2 is the invariant four-momentum transfer of the scattering and is defined as $Q^2 = -q^2 = -(\omega^2 - \vec{q}^2)$. For elastic electron scattering, $Q^2 = 4EE' \sin^2(\frac{\theta_e}{2})$

where θ_e is the electron scattering angle in the laboratory frame of reference.

Each Feynman diagram has an associated invariant amplitude, \mathcal{M}^{EM} or \mathcal{M}^{NC} . The amplitudes are summed to form the total first order invariant amplitude for the interaction, \mathcal{M} . The dominant amplitude is the electromagnetic interaction while the neutral weak interaction generates a small amplitude that is detectable via quantum interference. Because the weak interaction violates parity, the interference effects imply the existence of small pseudoscalar observables in electron scattering [BM01].

2.1 Nucleon Form Factors

The amplitude for the electromagnetic current (EC), following the notation of [Mus94], can be written as¹

$$\mathcal{M}^{EM} = \frac{4\pi\alpha}{q^2} Q_l l^\mu J_\mu^{EM}, \quad (2.1)$$

and the amplitude for the weak neutral current (NC) can be expressed as

$$\mathcal{M}^{NC} = -\frac{G_F}{2\sqrt{2}} (g_V^l l^\mu + g_A^l l^{\mu 5}) (J_\mu^{NC} + J_{\mu 5}^{NC}), \quad (2.2)$$

where Q_l , g_V^l , and g_A^l are the lepton electromagnetic, vector, and axial-vector charges respectively (Table 2.1). \mathcal{M}^{NC} shows no q^2 dependence because when $q^2 \ll M_{NC}$, the weak interaction is usually treated as a contact interaction with a strength determined by the Fermi constant [BPS04], $G_F \approx 1.166367(5) \times 10^{-5} \text{ GeV}^{-2}$ [Ams08].

¹One point of departure from the formalism of [Mus94] where $Q \equiv k - k'$. In this work $Q^2 \equiv -q^2 > 0$.

The lepton vector and axial-vector currents, l^μ and $l^{\mu 5}$ respectively, can be expressed as

$$l^\mu = \bar{u}_l \gamma^\mu u_l, \quad (2.3)$$

$$l^{\mu 5} = \bar{u}_l \gamma^\mu \gamma^5 u_l, \quad (2.4)$$

with μ_l representing the four-component lepton spinor, γ^μ ($\mu = 0, 1, 2, 3$) defining the Dirac matrices, with $\gamma^5 = i\gamma^0\gamma^1\gamma^2\gamma^3$. The fine structure constant is $\alpha = \frac{e^2}{4\pi}$ where e is the coupling strength of the electromagnetic interaction.² The Fermi constant [BM01] can be expressed as

$$G_F = \frac{e^2}{4\sqrt{2}M_W^2 \sin^2 \theta_W}, \quad (2.5)$$

where M_W is the mass of the W boson and θ_W is the weak mixing angle. The weak mixing angle can be related to the neutral and charged boson masses by the relation

$$\sin^2 \theta_W \equiv 1 - \frac{M_W^2}{M_Z^2}. \quad (2.6)$$

Fermion	Q_l	g_V^l	g_A^l
ν_e, ν_μ, ν_τ	0	1	-1
e^-, μ^-, τ^-	-1	$-1 + 4 \sin^2 \theta_W$	1
u, c, t	$\frac{2}{3}$	$1 - \frac{8}{3} \sin^2 \theta_W$	-1
d, s, b	$-\frac{1}{3}$	$-1 + \frac{4}{3} \sin^2 \theta_W$	1

Table 2.1: Electroweak charges of elementary fermions [Mus94]

Because the nucleon has internal structure, the hadronic currents include a set of form factors defined to encompass this complicated structure. Assuming gauge

²Unless otherwise noted, the equations in this work have been derived in a set of units where $\hbar c = 1$.

and Lorentz invariance, the hadronic vector currents of both the electromagnetic and weak interactions (one boson exchange) can be expressed as [HM84]

$$J_\mu^j = \bar{U}_N \left[F_1^j(q^2) \gamma^\mu + F_2^j(q^2) \frac{i\sigma^{\mu\nu} q_\nu}{2M} \right] U_N, \quad (2.7)$$

where U_N is a nucleon spinor, j denotes the type of interaction (γ /EM or Z /NC), $\sigma^{\mu\nu} = \frac{i}{2}[\gamma^\mu, \gamma^\nu]$, and N is the nucleon (p or n). The form factors F_1^j and F_2^j are the Dirac and Pauli form factors, respectively. They are normalized such that for the electromagnetic interaction, when $Q^2 = 0$,

$$F_1^\gamma(0) = Q_N, \quad (2.8)$$

$$F_2^\gamma(0) = \kappa_N, \quad (2.9)$$

where Q_N is the electric charge of the nucleon (in units of e), and κ_N is the anomalous magnetic moment of the nucleon (in units of the Bohr magneton).

There is an additional hadronic current to the neutral weak interaction due to the axial vector component. When this is included with the neutral weak vector current, the total hadronic current for the neutral weak interaction can be represented as

$$J_\mu^{NC} = \bar{U}_N \left[F_1^Z(q^2) \gamma^\mu + F_2^Z(q^2) \frac{i\sigma^{\mu\nu} q_\nu}{2M} + G_A^{eN} \gamma^\mu \gamma_5 \right] U_N, \quad (2.10)$$

where G_A^{eN} is the nucleon's neutral weak axial form factor.

In practice, it is frequently better to use a linear combination of $F_{1,2}$, known as the Sachs form factors expressed as [Sac62]

$$G_E^{jN} = F_1^{jN} - \tau F_2^{jN}, \quad (2.11)$$

$$G_M^{jN} = F_1^{jN} + F_2^{jN}. \quad (2.12)$$

Where $\tau = \frac{Q^2}{4M^2}$ and j is the interaction type, either γ for electromagnetic or Z for neutral weak. At $Q^2 = 0$, $G_E^{\gamma N}$ and $G_M^{\gamma N}$, are equivalent to the electric charge and magnetic moment of the nucleon, respectively. Additionally, in the Breit frame, or the center of mass frame defined by $\vec{p}' = -\vec{p}$, the Sachs form factors are the Fourier transforms of the nucleon charge and magnetic moment distributions [Sac62].

2.1.1 Flavor Decomposition

The hadronic currents, J_μ^{EM} , J_μ^{NC} , and $J_{\mu 5}^{NC}$, can also be expressed as

$$J_\mu^i \equiv \langle H | \hat{J}_\mu^i | H \rangle, \quad (2.13)$$

where $|H\rangle$ is any hadronic state, which in this case is either a proton or a neutron.

Assuming a point-like interaction between the gauge bosons (γ, Z) and the quarks internal to the nucleon, the quark current operators can be written as [Mus94]:

$$\hat{J}_\mu^{EM} \equiv \sum_q Q_q \bar{u}_q \gamma_\mu u_q, \quad (2.14)$$

$$\hat{J}_\mu^{NC} \equiv \sum_q g_V^q \bar{u}_q \gamma_\mu u_q, \quad (2.15)$$

$$\hat{J}_{\mu 5}^{NC} \equiv \sum_q g_A^q \bar{u}_q \gamma_\mu \gamma_5 u_q, \quad (2.16)$$

where the summation is over all quark flavors, which implicitly includes both quarks and their anti-quarks. The values of Q_q , g_V^q , and g_A^q given in Table 2.1. Expressing the quark current operators in this manner allows us to express the hadronic currents as

$$J_\mu^{EM} \equiv \bar{U}_N \sum_q Q_q \left[F_1^q \gamma^\mu + F_2^q \frac{i\sigma^{\mu\nu} q_\nu}{2M} \right] U_N, \quad (2.17)$$

$$J_\mu^{NC} \equiv \bar{U}_N \sum_q \left[g_V^q \left(F_1^q \gamma^\mu + F_2^q \frac{i\sigma^{\mu\nu} q_\nu}{2M} \right) + g_A^q G_A^q \gamma^\mu \gamma_5 \right] U_N, \quad (2.18)$$

where F_1^q , F_2^q , and G_A^q , are the Dirac, Pauli, and axial form factors, respectively, with quark flavor q . The quark form factors, F_1^q and F_2^q , are interaction independent and are the same in eqns. 2.17 and 2.18. Comparing eqns. 2.7 and 2.10 with eqns. 2.17 and 2.18 it is evident that the nucleon form factors $F_{1,2}^{\gamma N}$, $F_{1,2}^{ZN}$, and G_A^{eN} can be expressed in terms of the quark flavor form factors as

$$F_{1,2}^{\gamma N} = \sum_q Q_q F_{1,2}^q, \quad (2.19)$$

$$F_{1,2}^{ZN} = \sum_q g_v^q F_{1,2}^q, \quad (2.20)$$

$$G_A^{eN} = \sum_q g_A^q G_A^q, \quad (2.21)$$

where Q_q , g_v^q , and g_A^q are given in Table 2.1. This results in a set of five nucleon form factors in terms of 12 unknown quark form factors for each nucleon. The electromagnetic and neutral weak Sachs form factors can also easily be expressed as quark flavor form factors

$$G_{E,M}^{\gamma N} = \sum_q Q_q G_{E,M}^q, \quad (2.22)$$

$$G_{E,M}^{ZN} = \sum_q g_v^q G_{E,M}^q. \quad (2.23)$$

2.1.1.1 Flavor Vector Form Factors

Because the masses of the three heaviest quarks (c , b , and t) are greater than the mass of the proton, there is a strong suppression of their contributions to the properties of nucleons. This allows us to write the Sachs form factors in term of the

three lightest quark flavors

$$G_{E,M}^{\gamma N} = \frac{2}{3}G_{E,M}^{uN} - \frac{1}{3}(G_{E,M}^{dN} + G_{E,M}^{sN}) \quad (2.24)$$

$$G_{E,M}^{ZN} = \left(1 - \frac{8}{3}\sin^2\theta_W\right)G_{E,M}^{uN} - \left(1 - \frac{4}{3}\sin^2\theta_W\right)(G_{E,M}^{dN} + G_{E,M}^{sN}). \quad (2.25)$$

The number of unknowns can be further reduced by assuming charge symmetry which capitalizes on the fact that the (u, d) quarks in the proton **are in the same wave function** as the (d, u) quarks in the neutron [Mil98]. In addition, it is generally assumed that the strange quark distributions in the proton and the neutron are the same. These assumptions allow the following result.

$$G_{E,M}^{u,p} = G_{E,M}^{d,n} \equiv G_{E,M}^u, \quad G_{E,M}^{d,p} = G_{E,M}^{u,n} \equiv G_{E,M}^d, \quad G_{E,M}^{s,p} = G_{E,M}^{s,n} = G_{E,M}^s, \quad (2.26)$$

which reduces the number of unknowns and simplifies the notation. Charge symmetry breaking occurs due to the differing masses and charges of the u and d quarks, but this effect is generally less than 1% of the electromagnetic form factors [Mil98].

Explicitly writing the proton and neutron Sachs vector form factors using Eqns. (2.20 and 2.21) and charge symmetry yields

$$G_{E,M}^{\gamma p} = \frac{2}{3}G_{E,M}^u - \frac{1}{3}(G_{E,M}^d + G_{E,M}^s), \quad (2.27)$$

$$G_{E,M}^{\gamma n} = \frac{2}{3}G_{E,M}^d - \frac{1}{3}(G_{E,M}^u + G_{E,M}^s), \quad (2.28)$$

$$G_{E,M}^{Zp} = \left(1 - \frac{8}{3}\sin^2\theta_W\right)G_{E,M}^u - \left(1 - \frac{4}{3}\sin^2\theta_W\right)(G_{E,M}^d + G_{E,M}^s), \quad (2.29)$$

$$G_{E,M}^{Zn} = \left(1 - \frac{8}{3}\sin^2\theta_W\right)G_{E,M}^d - \left(1 - \frac{4}{3}\sin^2\theta_W\right)(G_{E,M}^u + G_{E,M}^s). \quad (2.30)$$

Rearranging Eqns. 2.27, 2.28, and 2.29, it is possible to express the proton's neutral

weak form factor as

$$G_{E,M}^{Zp} = (1 - 4 \sin^2 \theta_W) G_{E,M}^{\gamma p} - G_{E,M}^{\gamma n} - G_{E,M}^s. \quad (2.31)$$

This important results shows that a measurement of the neutral weak form factors, when combined with the well-known values for the electromagnetic form factors, provides a determination of the vector strange form factors.

2.1.1.2 Flavor Axial Form Factors

The neutral weak axial form factors can also be expressed as a sum of the individual quark flavor form factors, weighted by the weak axial charge of that flavor

$$G_A^{ZN} = g_A^u G_A^{uN} + g_A^d G_A^{dN} + g_A^s G_A^{sN}. \quad (2.32)$$

Assuming charge symmetry as well as the same strange quark distributions in protons and neutrons results in:

$$G_A^{up} = G_A^{dn} \equiv G_A^u, \quad G_A^{dp} = G_A^{un} \equiv G_A^d, \quad G_A^{sN} \equiv G_A^s, \quad (2.33)$$

and using the values in Table 2.1, the neutral weak axial form factors can be expressed in the following simplified manner

$$G_A^{Zp} = -(G_A^u - G_A^d) + G_A^s \quad (2.34)$$

$$G_A^{Zn} = (G_A^u - G_A^d) + G_A^s. \quad (2.35)$$

In the limit of “no strangeness”, the axial form factor has an explicit isovector structure:

$$G_A^Z = -(G_A^u - G_A^d) = -\tau_3 G_A \quad (2.36)$$

where $\tau_3 = +1$ (-1) for a proton (neutron). G_A can be related to the coupling constants g_A and g_V by $G_A(0) = -\frac{g_V}{g_A} = 1.2670 \pm 0.0035$ [Ams08] as determined from β -decay experiments [Mus94].

In the lowest order limit of single Z -boson exchange, the isovector and SU(3) singlet contributions survive:

$$G_A^Z = -\tau_3 G_A + G_A^s \quad (2.37)$$

where G_A^s is the strange quark contribution to nucleon spin. G_A^s comes from the axial vector strange matrix element $\langle p | \bar{s} \gamma_\mu \gamma_5 s | p \rangle$ measured in deep inelastic scattering experiments and discussed in section 2.3. Higher order corrections to G_A^s are expected to be significant and are also addressed in section 2.3.

2.1.1.3 Flavor Singlet Form Factors

The flavor decomposition may also be made in terms of the SU(3) flavor basis where the electromagnetic form factors are written as a sum of isovector and octet terms,

$$G_{E,M}^{\gamma p} = G_{E,M}^{3,p} + \frac{1}{\sqrt{3}} G_{E,M}^{8,p}. \quad (2.38)$$

The isovector form factor $G_{E,M}^{3,p}$ and the octet form factor, $G_{E,M}^{8,p}$ can be written in terms of individual quark contributions,

$$G_{E,M}^{3,p} = \frac{1}{2} (G_{E,M}^{u} - G_{E,M}^d) \quad (2.39)$$

$$G_{E,M}^{8,p} = \frac{1}{2\sqrt{3}} (G_{E,M}^u + G_{E,M}^d - 2G_{E,M}^s). \quad (2.40)$$

In this basis, the neutral weak form factors are

$$G_{E,M}^{Zp} = \left(\frac{1}{2} - \sin^2 \theta_w \right) G_{E,M}^{3,p} + \left(\frac{1}{2\sqrt{3}} - \frac{1}{\sqrt{3}} \sin^2 \theta_w \right) G_{E,M}^{8,p} - \frac{1}{4} G_{E,M}^0, \quad (2.41)$$

$$G_{E,M}^{Zp} = \left(\frac{1}{2} - \sin^2 \theta_w \right) G_{E,M}^{\gamma,p} - \frac{1}{4} G_{E,M}^0, \quad (2.42)$$

where

$$G_{E,M}^{0p} = \frac{1}{3} (G_{E,M}^u + G_{E,M}^d + G_{E,M}^s) \quad (2.43)$$

is the flavor singlet form factor. A measurement of $G_{E,M}^{Zp}$, as taken during the G^0 experiment, when combined with the known values for the proton's electromagnetic form factors, determines the flavor singlet form factor, $G_{E,M}^{0p}$. This is the origin of the name of the G^0 experiment.

2.2 Parity Violation in Electron Scattering

It was Kaplan and Manohar in 1988 [KM88] who first showed that information about strange quark effects in the nucleon could be extracted from elastic neutral current processes. They were followed by Beck [Bec89] and McKeown [McK89]  who showed how $G_{E,M}^Z$ could be measured using parity-violating electron scattering, which led to a series of experimental programs. These experiments include the G^0 Backward Angle measurement at Jefferson Lab's Continuous Electron Beam Facility (CEBAF), which is the topic of this thesis, and several others that are described and discussed in Chap. 3.

2.2.1 Experimental Observables: Neutral Weak Vector Form Factors

As previously mentioned, the total invariant amplitude for e-N elastic or quasi-elastic scattering is a coherent sum of the electromagnetic and neutral current amplitudes

$$\mathcal{M} = \mathcal{M}^{EM} + \mathcal{M}^{NC}, \quad (2.44)$$

where leading order values of \mathcal{M}^{EM} and \mathcal{M}^{NC} are given in Eqns. 2.1 and 2.2 respectively. The scattering probability, $d\sigma$, is proportional to the total invariant amplitude squared

$$d\sigma \propto |\mathcal{M}|^2 \propto |\mathcal{M}^{EM}|^2 + 2\mathcal{M}^{EM*} \mathcal{M}^{NC} + |\mathcal{M}^{NC}|^2, \quad (2.45)$$

where \mathcal{M}^{EM*} represents the complex conjugate of \mathcal{M}^{EM} . The neutral weak amplitude is strongly suppressed relative to the electromagnetic amplitude in an absolute cross section measurement. Therefore, in order to measure the neutral weak vector form factors, it is necessary to take advantage of the parity-violating nature of the weak interaction. Because the weak interaction violates parity while the electromagnetic interaction does not, it is the interference term, $2\mathcal{M}^{EM*} \mathcal{M}^{NC}$, that is the cause of the parity violation seen in e-N elastic and quasi-elastic scattering.

Operators formed from a vector and an axial vector operator are parity-violating while operators formed from squares of either conserve parity. The parity-violating component of the neutral current amplitude arises from the cross terms of the axial and vector currents. The amplitude can be written as a sum of parity-conserving \mathcal{M}_{PC}^{NC} and parity-violating \mathcal{M}_{PV}^{NC} amplitudes:

$$\mathcal{M}_{PC} = -\frac{G_F}{2\sqrt{2}}(g_V^l l^\mu J_\mu^{NC} + g_A^l l^{\mu 5} J_{\mu 5}^{NC}), \quad (2.46)$$

$$\mathcal{M}_{PV} = -\frac{G_F}{2\sqrt{2}}(g_V^l l^{\mu 5} J_\mu^{NC} + g_A^l l^\mu J_{\mu 5}^{NC}). \quad (2.47)$$

Parity violation can be probed using longitudinally polarized electrons where the two states of electron polarization (parallel or anti-parallel to the beam) correspond to the two parity states. The parity-violating asymmetry for the scattering of the polarized electrons from a target of unpolarized protons is defined as the difference in the cross section for each helicity state, divided by the sum of the cross sections:

$$A \equiv \frac{\sigma_+ - \sigma_-}{\sigma_+ + \sigma_-}. \quad (2.48)$$

Eliminating the parity conserving terms, and any terms with G_F^2 in the numerator or G_F in the denominator, provides the following expression for the parity-violating asymmetry:

$$A \approx 2 \frac{\mathcal{M}^{EM*} \mathcal{M}^{PV}}{|\mathcal{M}^{EM}|^2}. \quad (2.49)$$

Substituting in Eqns. 2.1, 2.7, 2.10, 2.11, 2.12, and 2.47 and rearranging the terms as in Refs. [RS74] and [BPS04] yields:

$$A = -\frac{G_F Q^2}{4\pi\alpha\sqrt{2}} \frac{A_E + A_M + A_A}{[\epsilon(G_M^\gamma)^2 + \tau(G_M^\gamma)^2]}, \quad (2.50)$$

with the electric, magnetic, and axial components of the asymmetry expressed as;

$$A_E = \epsilon G_E^Z(Q^2) G_E^\gamma(Q^2), \quad (2.51)$$

$$A_M = \tau G_M^Z(Q^2) G_M^\gamma(Q^2), \quad (2.52)$$

$$A_A = -(1 - 4 \sin^2 \theta_W) \sqrt{\tau(1 + \tau)(1 - \epsilon^2)} G_A^e(Q^2) G_M^\gamma(Q^2), \quad (2.53)$$

and

$$\tau = \frac{Q^2}{4M_N^2} \quad \text{and} \quad \epsilon = \frac{1}{1 + 2(1 + \tau) \tan^2 \frac{\theta}{2}}. \quad (2.54)$$

Writing the asymmetry expression in the above manner clearly shows the $\gamma-Z$ interference and the sensitivity of the electric, magnetic, and axial form factors to the kinematics of the experiment. In general, forward angle experiments are sensitive to a combination of A_E and A_M and backward angle experiments to a combination of A_M and A_A . Additionally, quasielastic scattering from an isospin 0 target, such as a deuteron can be used to enhance A_A [BPS04].

The notation for the axial form factor has been modified here from G_A^Z to G_A^e in order to distinguish the ~~from~~ factor as seen by electron scattering from that seen by neutrino scattering where the higher order diagrams involving electromagnetic interactions are absent. This will be discussed in more detail in section 2.3.

2.2.2 Electroweak Radiative Corrections to the Neutral Current

The neutral weak vector and axial vector form factors derived at leading order in Section 2.1.1.1 require corrections due to higher order electroweak processes. These corrections modify the coupling constants at the interaction vertex and in effect, modify the weak vector and axial charges. The corrections fall in one of three categories: one quark, many-quark, and heavy quark renormalization. One quark radiative corrections that do not require knowledge of quark interactions can be calculated using Standard Model electroweak theory with small associated uncertainties. The electroweak calculations require a renormalization scheme to be

selected, and in this work, the “MS-bar” (\overline{MS}) or modified minimal subtraction scheme is used. The weak mixing angle in this scheme is no longer defined as it was in Eqn. 2.6, but now carries a dependence on a renormalization mass scale μ [Mus94], which in this case is the mass of the Z boson, $M_Z = 91.1876 \pm 0.0021$ GeV [Ams08].

For the vector weak form factors at low momentum transfers, the one quark corrections have a weak dependence on Q^2 and have the same $(1 - 4 \sin^2 \theta_W)$ multiplier as the tree-level amplitudes and therefore, despite being the dominate higher-order vector correction, are typically very small [BPS04]. One-quark axial corrections are also calculable with small errors, but unlike the vector correction, it is substantial compared to the tree-level amplitudes. The biggest effect of electroweak radiative corrections however, is the many-quark correction to the axial term. Corrections involving many-quarks where strong interactions are included, can

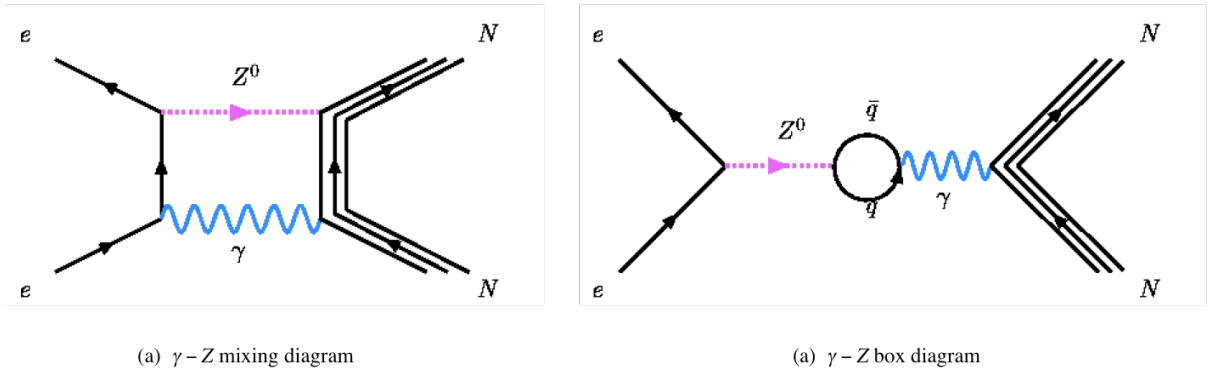


Figure 2.2: *Representative one-quark Feynman diagrams contributing to electroweak radiative corrections.*

not be easily calculated because Perturbative Quantum Chromodynamics (PQCD) is not effective in the energy range of the G^0 measurements, ≈ 1 GeV. These cor-

rections have a large associated uncertainty because of our inability to include all virtual hadronic states in the calculation. It should be noted that the many-quark correction only effects the axial contribution. 

The third correction is heavy quark renormalization. When the neutral weak form factors were decomposed into quark form factors (Eqns. 2.27, 2.28, 2.29, and 2.30) only the three lightest quark flavors were included. Heavy-quark renormalization of the light-quark current operators results in corrections to the neutral current couplings. These corrections were calculated by Kaplan and Manohar [KM88] and were found to be small, with the vector term on the order of 10^{-4} and 10^{-2} for the axial term. These corrections are neglected in this work due to their small size.

Electroweak radiative effects can be parametrized in terms of the parameters ρ and κ as proposed in the pioneering work of Marciano and Sirlin, [MS84]. In this approach, the proton's weak charge becomes

$$Q_w = 1 - 4 \sin^2 \theta_W \rightarrow \rho(1 - 4\kappa \sin^2_{\theta_W}). \quad (2.55)$$

Using this parameterization, the proton asymmetry can be written as a sum of vector, strange vector, and axial vector contributions [TBM09],

$$A_p = - \left(\frac{G_F Q^2}{4\sqrt{2}\pi\alpha} \right) (A_V + A_s + A_A), \quad (2.56)$$

where

$$A_V = \rho \left[(1 - 4\kappa \sin^2_{\theta_W}) - \frac{\epsilon G_E^{\gamma,p} G_E^{\gamma,n} + \tau G_M^{\gamma,p} G_M^{\gamma,n}}{\sigma} \right], \quad (2.57)$$

$$A_s = -\rho \frac{\epsilon G_E^{\gamma,p} G_E^s + \tau G_M^{\gamma,p} G_M^s}{\sigma}, \quad (2.58)$$

$$A_A = -(1 - 4 \sin^2_{\theta_W}) \sqrt{\tau(1 + \tau)(1 - \epsilon^2)} \frac{G_A^e G_M^{\gamma,p}}{\sigma}, \quad (2.59)$$

with $\sigma = \epsilon(G_E^{\gamma,p})^2 + \tau(G_M^{\gamma,p})^2$ representing the unpolarized proton cross section. The form factor G_A^e implicitly contains higher order radiative corrections for the proton axial current and is discussed in Section 2.3.

An alternative parameterization is in terms of isoscalar and isovector weak radiative corrections for the vector form factors. The proton and neutron radiative corrections are given to first order in $\rho - 1$ and $\kappa - 1$ by

$$R_V^p = \rho - 1 - (\kappa - 1) \frac{4 \sin^2 \theta_W}{1 - 4 \sin^2 \theta_W}, \quad (2.60)$$

$$R_V^n = \rho - 1. \quad (2.61)$$

The first order neutral vector form factor was given in Eqn. 2.31. The full expression for $G_{E,M}^Z$, including the electroweak radiative corrections is [BPS04]

$$G_{E,M}^{Zp} = (1 - 4 \sin^2 \theta_W) (1 + R_V^p) G_{E,M}^{\gamma p} - (1 + R_V^n) G_{E,M}^{\gamma n} - G_{E,M}^s. \quad (2.62)$$

The full asymmetry for a nucleon, N , in terms of the vector R parameters can be written as [Mus94][LMRM07]:

$$\begin{aligned} A_N = & - \frac{G_F Q^2}{4\pi\alpha\sqrt{2}} \frac{1}{[\epsilon(G_E^N)^2 + \tau(G_M^N)^2]} \\ & \times \{ (\epsilon(G_E^N)^2 + \tau(G_M^N)^2)(1 - 4 \sin^2 \theta_W)(1 + R_V^p) \\ & - (\epsilon G_E^p G_E^n + \tau G_M^p G_M^n)(1 + R_V^n) \\ & - (\epsilon G_E^N G_E^s + \tau G_M^N G_M^s)(1 + R_V^{(0)}) \\ & - (1 - 4 \sin^2 \theta_W) \epsilon' G_M^N G_A^e \}. \end{aligned} \quad (2.63)$$

2.3 Axial Form Factor and the Anapole Moment

As previously mentioned, in neutrino-nucleon scattering, G_A^Z is a very good approximation of the axial form factor. In electron scattering however, electroweak radiative corrections to the axial current are a large effect. For clarity, the notation $G_A^e \equiv G_A^Z$ is used to denote the radiatively corrected axial form factor seen in electron scattering.

Including higher order electroweak corrections in the expression for the axial form factor, modifies Eqn. 2.37 in the following manner [BPS04];

$$G_A^e = -\tau_3 (1 + R_A^{T=1}) G_A + \sqrt{3} R_A^{T=0} G_A^8 + G_A^s (1 + R_A^{(0)}). \quad (2.64)$$

There is now a term proportional to an SU(3) isoscalar octet form factor G_A^8 , which at tree level is zero. The isovector term G_A may be written as

$$G_A = \left(\frac{g_A}{g_V} \right) G_D \quad (2.65)$$

where

$$G_D(Q^2) = \frac{1}{(1 + Q^2/M_A^2)^2} \quad (2.66)$$

uses a dipole form to parametrize the Q^2 dependence of G_A . The ratio of the axial and vector coupling constants, $\frac{g_A}{g_V} = 1.2695(29)$ [Ams08], is well known at zero momentum transfer from β -decay and other charged-current weak interaction processes, such as $\nu_\mu + n \rightarrow p + \mu^-$ from quasi-elastic neutrino scattering from deuterium. The axial mass, $M_A = 1.014 \pm 0.014$ (GeV/c)², was determined by fitting neutrino-deuterium data and comparing that result with calculations from pion electroproduction experiments corrected for hadronic effects [BABB08]. The pion

and the neutrino data are in close agreement, so although M_A can not at this time be determined from first principles, it can be described accurately phenomenologically for $Q^2 < 1$ (GeV/c)².

The dipole expression of G_A can then be used to determine an axial radius in a low momentum expansion of G_A with Q^2 [Bei05], 

$$\langle r_A^2 \rangle = \frac{6}{g_A} \frac{dG_A}{dQ^2} \Big|_{Q^2=0} = \frac{12}{M_A}. \quad (2.67)$$

The SU(3) octet form factor G_A^s at $Q^2 = 0$ can be estimated from the ratio of axial vector to vector couplings in hyperon β decay which, assuming SU(3) flavor symmetry, can be related to the hyperon F and D coefficients [Bei05] [Got00],

$$G_A^s(0) = \frac{(3F - D)}{2\sqrt{3}} = 0.585 \pm 0.025. \quad (2.68)$$

The isoscalar strange axial form factor G_A^s reduces at $Q^2 = 0$ to $G_A^s = \Delta s$ where Δs is the fraction of nucleon spin carried by the strange quarks ($s + \bar{s}$). The Q^2 behavior of both G_A^s and G_A^s has not been measured. Generally, it's assumed to have the same dipole form as the isovector form factor G_A , resulting in the following expression for the axial form factor,

$$G_A^e = G_A^D \left[\frac{G_A}{G_V} \tau_3 (1 + R_A^{T=1}) + \frac{3F - D}{2} R_A^{T=0} + \Delta s (1 + R_A^{(0)}) \right]. \quad (2.69)$$

2.3.0.1 The Anapole Contribution

The anapole moment is a parity-violating electromagnetic interaction where along with a photon exchange between the electron and the nucleon, a weak parity-violating hadronic interaction also occurs [ZPHRM00]. The electroweak radiative

correction associated with the anapole moment was referred to earlier as the “many quark” correction to the axial form factor. Zhu calculated the contributions of the anapole moment to $R_A^{T=1}$ and $R_A^{T=0}$ using heavy baryon chiral perturbation theory to order p^3 [ZPHRM00]:

$$R_A^{T=1}|_{anapole} = -\frac{8\sqrt{2}\pi\alpha}{G_\mu\Lambda_\chi^2} \frac{1}{1-4\sin^2\theta_W} \frac{a_s}{g_A}, \quad (2.70)$$

$$R_A^{T=0}|_{anapole} = -\frac{8\sqrt{2}\pi\alpha}{G_\mu\Lambda_\chi^2} \frac{1}{1-4\sin^2\theta_W} \frac{a_v}{g_A}, \quad (2.71)$$

where $\Lambda_\chi = 4\pi F_\pi$ is the chiral symmetry breaking scale and the anapole moment is given by the quantity $a_s + \tau_3 a_v$. The relative importance of the anapole interaction is clearly seen in the $\frac{1}{1-4\sin^2\theta_W} \approx 10$ enhancement to the correction.

Liu, Mckeown, and Ramsey-Musolf [LMRM07] calculated  the isovector and isoscalar electroweak axial radiative corrections (Table 2.2) following [ZPHRM00] and [Mus94]. Their result shows that the theoretical uncertainty in the total R_A is large compared to the one-quark corrections, demonstrating the importance of measuring G_A^e during the G^0  backangle experiment and constraining $R_A^{T=1}$.

	$R_A^{T=1}$	$R_A^{T=0}$
One quark	0.172	-0.253
Many quark	-0.086(0.34)	0.014(0.19)
Total	-0.258(0.34)	-0.239(0.20)

Table 2.2: The “one quark”, “many quark”, and total corrections to the axial charges in the \overline{MS} scheme.

2.4 The Deuteron

In order to determine G_A^e , G_E^S , and G_M^S experimentally, the three unknowns requiring a measurement are G_E^Z , G_M^Z , and G_A^Z (see Eqn. 2.63). Two asymmetry measurements can be made using a proton target but with two different kinematic settings, i.e. forward angle or backward angle scattering. Another equation with the same unknowns and same Q^2 is also required. **Using a target of neutrons would be ideal.** Although a neutron target isn't feasible, a deuterium target is.

In the static approximation, the nucleons in the deuteron are treated as free, non-interacting particles. The proton and neutron asymmetries add incoherently, resulting in the following expression for the parity violating asymmetry from quasi-elastic electron scattering from deuterium, A_d [HPD92]:

$$A_d = \frac{\sigma_p A_p + \sigma_n A_n}{\sigma_p + \sigma_n}, \quad (2.72)$$

where $\sigma_{n(p)}$ is the cross section for elastic electron-neutron (proton) scattering.

Because of the τ_3 term in front of the $R_A^{T=1}$ in Eqn. 2.69, and the relative size of $G_M^p \approx 2.79$ and $G_M^n \approx -1.91$, the $R_A^{T=1}$ term is enhanced, and the $R_A^{T=0}$ term is suppressed in the deuterium asymmetry measurement.

2.4.0.2 Two Boson Exchange Correction

Because the expected size of the extracted strange vector form factors is small and because the proton's weak charge is also small, the relative importance of two boson exchange (TBE) effects in a parity-violating electron scattering measurement are enhanced [TBM09]. Although a suppressed, higher order interaction, two-photon

exchange (TPE) ~~was found~~ to have a significant impact in resolving the discrepancy between the electric to magnetic proton form factor ratio measurements using the Rosenbluth separation technique [BMT05].

Tjon, Blunden and Melnitchouk have recently calculated the electroweak radiative corrections including corrections arising from the interference of first order and TBE diagrams, both electromagnetic (γ, γ) and electroweak(γ, Z). The calculation was made by changing the amplitudes in Eqn. 2.45 in the following manner,

$$\mathcal{M}^{EM} \rightarrow \mathcal{M}^{EM} + \mathcal{M}^{\gamma\gamma}, \quad (2.73)$$

$$\mathcal{M}^{NC} \rightarrow \mathcal{M}^{NC} + \mathcal{M}^{\gamma Z} + \mathcal{M}^{Z\gamma}, \quad (2.74)$$

where the two-photon and γZ exchange amplitudes are given explicitly in [TBM09]. The relative corrections from the $Z(\gamma\gamma), \gamma(\gamma Z)$, and $\gamma(\gamma\gamma)$ interference terms are identified as [TBM09]

$$\delta_{Z(\gamma\gamma)} = \frac{2\mathcal{R}(\mathcal{M}^{Z*}\mathcal{M}^{\gamma\gamma})}{2\mathcal{R}(\mathcal{M}^{Z*}\mathcal{M}^{\gamma})}, \quad (2.75)$$

$$\delta_{\gamma(\gamma Z)} = \frac{2\mathcal{R}(\mathcal{M}^{\gamma*}\mathcal{M}^{\gamma Z} + \mathcal{M}^{\gamma*}\mathcal{M}^{Z\gamma})}{2\mathcal{R}(\mathcal{M}^{\gamma*}\mathcal{M}^Z)}, \quad (2.76)$$

$$\delta_{\gamma(\gamma\gamma)} = \frac{2\mathcal{R}(\mathcal{M}^{\gamma*}\mathcal{M}^{\gamma\gamma})}{|\mathcal{M}^{\gamma}|^2}. \quad (2.77)$$

In order to apply their TBE correction, it is necessary to first remove the $Q^2 = 0$ hadronic, or low-mass portion of the TBE in the terms ρ and κ which are then used to calculate the R factor corrections [TBM09]. The low-mass portion of the corrections are referred to as $\Delta\rho_{MS}$ and $\Delta\kappa_{MS}$; these values are shown in Table 2.3 and details of the calculation are provided in Sec. 2.5.

The correction to Eqn. 2.59 is then

$$A = (1 + \delta)A^0 \equiv \left(\frac{1 + \delta_{Z(\gamma\gamma)} + \delta_{\gamma(Z\gamma)}}{1 + \delta_{\gamma(\gamma\gamma)}} \right) A^0 \quad (2.78)$$

where A^0 is given in Eqn. 2.63.

2.5 Electroweak Parameters

This section presents a summary of the parameters and calculations used to determine the electroweak correction parameters, the R factors, which were applied to the G^0 backward angle measurement to extract the axial and vector strange form factors. All values are calculated in the \overline{MS} scheme.

Quantity	Value	Reference
G_F	1.16639×10^{-5}	[Ams08]
M_A	$1.014 \pm 0.014 \text{ (GeV/c)}^2$	[BABB08]
\hat{s}_Z^2	0.23120(15)	[Ams08]
g_A	1.2695 ± 0.0029	[Ams08]
$3F - D$	0.585 ± 0.025	[Ams08]
g_A	1.2695 ± 0.0029	[Got00]
ρ_1	0.9875	[Ams08]
ρ_2	1.0004	[Ams08]
κ_1	1.0025	[Ams08]
κ_2	1.0298	[Ams08]
λ_{1u}	-1.80×10^{-5}	[Ams08]
λ_{1d}	3.6×10^{-5}	[Ams08]
λ_{2u}	-0.0121	[Ams08]
λ_{2d}	0.0026	[Ams08]
$\Delta\rho_{MS}$	-0.00071	[TBM09]
$\Delta\kappa_{MS}$	-0.001027	[TBM09]

Table 2.3: *Parameters used to calculate the electroweak radiative corrections.*

To arrive at the R factors, the values in Table 2.3 are used to first calculate a set of constants, C_{1u}, C_{1d}, C_{2u} , and C_{2d} (Eqn. 2.79) found in the Particle Data

Book (PDG) that describe the coupling of the electron current to the quark current [Ams08]. These relations are:

$$\begin{aligned}
C_{1u} &= \rho_1^* \left(-\frac{1}{2} + \frac{4}{3} \kappa_1^* \hat{s}_Z^2 \right) + \lambda_{1u}, \\
C_{1d} &= \rho_1^* \left(\frac{1}{2} - \frac{2}{3} \kappa_1^* \hat{s}_Z^2 \right) + \lambda_{1d}, \\
C_{2u} &= \rho_2^* \left(-\frac{1}{2} + 2\kappa_2^* \hat{s}_Z^2 \right) + \lambda_{2u}, \\
C_{2d} &= \rho_2^* \left(\frac{1}{2} - 2\kappa_2^* \hat{s}_Z^2 \right) + \lambda_{2d},
\end{aligned} \tag{2.79}$$

where $\rho_i^* = \rho_i - \Delta\rho_{MS}$ and $\kappa_i^* = \kappa_i - \Delta\kappa_{MS}$. The the axial and vector quark charges can be expressed in terms of the C parameters, Eqn. 2.80. The quark charges are related to the R factors through the six weak nucleon charges, Eqn. 2.81.

$$\begin{aligned}
c_V^{u,c,t} &= -2C_{1u}, & c_V^{d,s,b} &= -2C_{1d}, \\
c_A^{u,c,t} &= \frac{2C_{2u}}{1 - 4\sin^2\theta_w}, & c_A^{d,s,b} &= \frac{2C_{2d}}{1 - 4\sin^2\theta_w},
\end{aligned} \tag{2.80}$$

And finally, the six weak nucleon charges provide the link between the quark charges and the R factors,

$$\begin{aligned}
Q_W^p &= 2c_V^u + c_V^d = (1 + R_V^p)(1 - 4\sin^2\theta_w), \\
Q_W^n &= 2c_V^d + c_V^u = -(1 + R_V^n), \\
Q_W^{(0)} &= c_V^u + c_V^d + c_V^s = -(1 + R_V^0), \\
Q_A^{T=1} &= \frac{1}{2}(c_A^u - c_A^d) = -(1 + R_A^{T=1}), \\
Q_A^{T=0} &= \sqrt{3}(c_A^u + c_A^d) = \sqrt{3}(1 + R_A^{T=0}), \\
Q_A^{(0)} &= c_A^u + c_A^d + c_A^s = (1 + R_A^0).
\end{aligned} \tag{2.81}$$

Table 2.4 shows the values for the R factors (“one quark” only) for hydrogen.

R Factor	Value
R_V^p	-0.043
R_V^n	-0.0124
$R_V^{(0)}$	-0.0124
$R_A^{T=1}$	-0.171
$R_A^{T=0}$	-0.253
$R_A^{(0)}$	-0.550

Table 2.4: *Radiative correction factors (“one quark”)*.

2.6 Theoretical Predictions of G_E^S and G_M^S

The G^0 measurement of the vector strange form factors is independent of any theoretical models predicting the presence or behavior of strange quarks in the nucleons. One can argue that this makes the theoretical predictions even more interesting. The difficulty in calculating static properties of the nucleon is that the strong coupling constant (α_s) is large at low energies and therefore it’s not possible to use a perturbative expansion in α_s to describe the interaction. Because of the difficulty in a straight-forward calculation of the strange quark contribution to nucleon properties, there have been a wide variety of approaches to making an effective calculation. A survey of the most popular methods is presented below.

Most theories focus on predicting the contribution to the strange magnetic moment, μ_s , and the strangeness radius, r_s , both defined at $Q^2 = 0$. The strangeness radius gives the mean square radius of the strange “charge” distribution. A positive value implies that the s quark is further away from the center of the nucleon than

\bar{s} and visa versa [BH01]. The expressions for these quantities are:

$$\mu_s = G_M^s(Q^2 = 0) \quad (2.82)$$

$$\langle r_s \rangle \equiv -6 \frac{dG_E^s}{dQ^2}(Q^2 = 0) \quad (2.83)$$

2.6.1 Chiral Perturbation Theory

Chiral perturbation theory (CHPT) is a powerful tool that capitalizes on the QCD Lagrangian having an approximate $SU(3)_L \times SU(3)_R$ symmetry in the limit where the light quark masses vanish. Because the physical masses of the three lightest quarks are much less than the hadronic scale (≈ 1 GeV), the massless approximation is reasonable. Chiral symmetry is used to relate one set of observables to another, or to draw on one set of measured quantities to predict another [RMI97].

This strategy breaks down in the flavor-singlet channel because the coefficients of the relevant flavor-singlet operators in the chiral Lagrangian, which contain information on short-distance hadronic effects, cannot be determined from existing measurements using chiral symmetry [RMI97]. Leading order, long-distance contributions are calculable however for μ_s and r_s , but it is not clear that these contributions dominate the short-distance effects. Therefore in order to determine the strangeness contribution of the nucleon, model-dependent assumptions are necessary [RMI97].

There are a number of hadronic models, but two that will be discussed here are variations of “pole” and the “loop” models. The primary shared feature of these models is the use of a strange intermediate hadronic state to approximate the

nucleon's strangeness content.

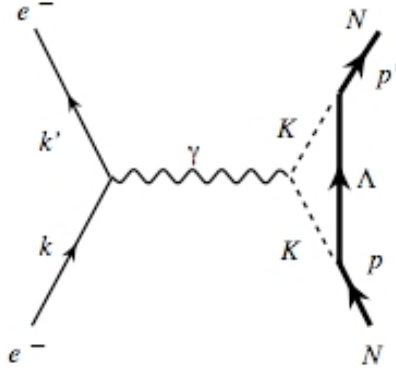


Figure 2.3: *The primary feynman diagram for a loop-model calculaton.*

2.6.1.1 Loop Models

In the Kaon Loop model, also referred to as the kaon cloud model, a nucleon combines with a $q\bar{q}$ pair to form a meson and an intermediate baryon state (see Fig. 2.3). The $q\bar{q}$ pair annihilates when the meson and baryon recombine leaving the original nucleon. One of the appeals of this model is the physical interpretation of the nucleon charge radius, where the model characterizes a spatial asymmetry with a non-zero charge distribution for s and \bar{s} . The intermediate strange meson-baryon state (typically modeled as a kaon and a hyperon) allows the s and \bar{s} to spatially separate because of the mass difference between the two intermediate state particles [RMI97]. Another motivation for this model came from the success of a pion loop calculation of the nucleon's electromagnetic form factors carried out by Bethe and DeHoffman [BH55]. When their results were reported, there was surprising agreement with experimental values for both the nucleon's charge radii

and magnetic moments, despite the large πN coupling which enters the perturbative calculation. This led to the belief that the pion cloud dominates the nucleon's isovector electromagnetic moments and that it is sufficiently described using a one-loop calculation. It was thought that if this ~~was~~ also the case for the strangeness sector, then the kaon cloud would provide the dominant contribution to the strange charge and magnetic moment [RMI97].

One approach for using kaon loop calculations was made by Koepf, Henley, and Pollock [KHP92]. They used bag models, both the “cloudy” constituent quark model and the cloudy bag model (CBM) to describe the hadrons. The size and structure of the nucleon bag was contained in a form factor, $v(k)$, with the size of the bag serving as the only unknown parameter. The model bag size was extracted using fits to the nucleon magnetic moments and charge radii. After fixing the size parameter, kaon loop calculations were completed.

Kaon loops introduce divergences that are typically handled with a momentum cut-off in the loop integral [DGH92]. Ramsey-Musolf and Burkardt performed a loop calculation within the context of the SU(3) linear σ model where the leading strangeness moments are ultraviolet finite. The calculation was performed by including hadronic form factors at the meson-nucleon vertices, using results of fits to baryon-baryon scattering in the one meson exchange approximation [MB94].

Geiger and Isgur [GI97] provided a follow-on kaon loop calculation using a non-relativistic quark model with yet another variation. Their calculation summed over a complete set of strange intermediate states, rather than just a few low-lying states, which provided a consistency with the OZI rule. The authors point out

that their results are not predictive of μ_s because their calculation ignored pure OZI-forbidden effects.

2.6.1.2 Pole Models

Based on analyticity and causality, dispersion relations (DR) relate the real parts of the form factors to integrals involving their imaginary parts. The imaginary parts, or spectral functions, contain information on the contributions to the form factor dynamics made by various states in the hadronic spectrum [HRM99].

For example, to obtain the dispersion relation for the Dirac form factor, $F_i(t)$, where t is real, the assumption is made that an analytic continuation $F_i(z)$ exists in the upper-half plane that approaches $F_i(t)$ as $z \rightarrow t + ie$ and that $\frac{F_i(z)}{z^n} \rightarrow 0$ as $z \rightarrow \infty$ for non-negative integers in the upper-half plane. Using Cauchy's theorem, a subtracted DR is shown for F_1 and an unsubtracted one for the Pauli form factor, F_2 :

$$F_1(t) = F_1(0) + \frac{t}{\pi} \int_{9m_\pi^2}^{\infty} \frac{ImF_1(t')}{t'(t'-t)} dt', \quad (2.84)$$

$$F_2(t) = \int_{9m_\pi^2}^{\infty} \frac{ImF_2(t')}{t'(t'-t)} dt'. \quad (2.85)$$

The lower limit of integration is given by the threshold of the lightest intermediate state contributing to the form factors, the 3π state [HRM99].

Poles models take a dispersion analysis approach, and are based on the work of Höller et al., [H76], where the basic premise is that the exchanged boson fluctuates into an isoscalar meson, either an ω or a ϕ , and then the meson interacts with the

nucleon (see Fig. 2.4). Both the ω and the ϕ are linear combinations of strange and

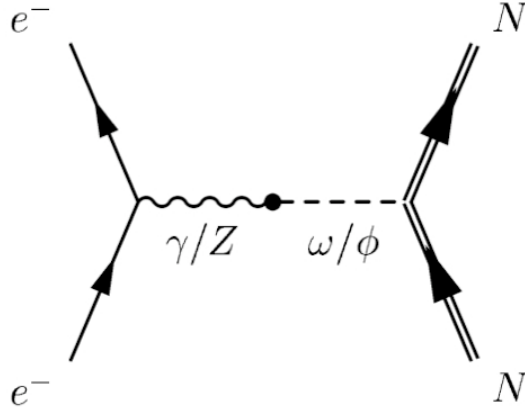


Figure 2.4: *The primary feynman diagram for a pole-model calculaton.*

non-strange base states:

$$|\omega\rangle = \cos(\eta)|\omega_o\rangle - \sin(\eta)|\phi_o\rangle, \quad (2.86)$$

$$|\phi\rangle = \sin(\eta)|\omega_o\rangle + \cos(\eta)|\phi_o\rangle, \quad (2.87)$$

where $\phi_o = |s\bar{s}\rangle$, $\omega_o = \frac{1}{\sqrt{2}}(|u\bar{u}\rangle + |d\bar{d}\rangle)$, and $\eta = 0.053 \pm 0.005$ is the mixing angle [Jaf89].

Vector meson dominance (VMD) is a special application of a dispersion relation with the assumption that the nucleon matrix element can be written as a summation over intermediate vector states. For example,

$$F_1^a(q^2) = F_1^a + \sum_V \frac{q^2 a_V^a}{m_V^2 - q^2}, \quad (2.88)$$

$$F_2^a(q^2) = \sum_V \frac{m_V^2 b_V^a}{m_V^2 - q^2}, \quad (2.89)$$

where m_V is the mass of an intermediate meson V . Jaffe calculated the strangeness radius and magnetic moment using a 3-pole fit to experimental data for the spectral

function of the isoscalar nucleon form factors. His first and second terms represented the coupling of nucleons to $\omega(780)$ and $\phi(1020)$ mesons. The third term represented contributions from other mass states.

2.6.1.3 Loops and Poles

Loop and pole predictions for the strangeness radius are opposite sign, and the magnitude of the loop prediction for the strangeness radius is about 20 times smaller for the Dirac radius than that of the pole prediction. This motivated Cohen, Forkel, and Nielsen to attempt to establish a link between the pole and loop pictures, by combining the VMD model in the ω and ϕ sector ($YT = 0, J^{PC} = 1^{--}$) with Musolf and Burkardt's loop calculation. They calculated the nucleon strange matrix elements using kaon loops, and used Höller's empirical fits for the isoscalar matrix elements, which were then combined using the VMD assumption with only ω and ϕ poles [CFN93].

2.6.2 Lattice QCD

Lattice QCD is a non-perturbative computational method based on a Feynman path integral approach to quantum field theory. Computations are performed on a lattice of space-time through intensive use of numerical integrations. Quarks and gluons reside on lattice points and can only travel along lines between them. This approximation approaches continuum QCD as the spacing between the lattice points approaches zero.

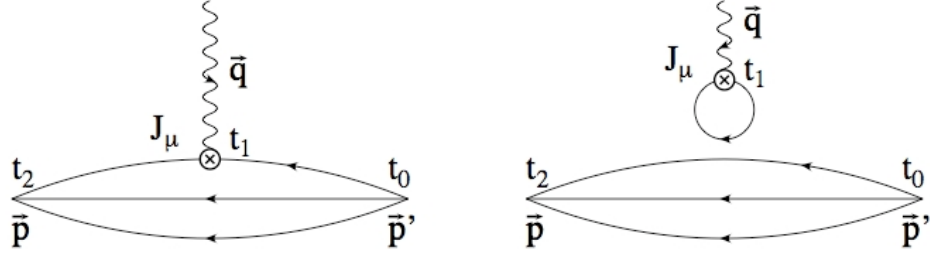


Figure 2.5: *Three point function representations. The connected insertion (left) compared to the disconnected insertion (right) [Doi09].*

Unlike the models previously discussed, lattice QCD offers a first-principle calculation. One of the major difficulties with using lattice calculations to calculate the strange electromagnetic form factors, is that the calculation requires the evaluation of the disconnected insertion (DI). The DI calculation (Fig. 2.5 (right)) is a much more difficult calculation compared to the connected insertion (Fig. 2.5 (left)) calculation, because the straightforward DI calculation requires all-to-all propagators, and is prohibitively expensive, [Doi09]. Recently, Doi et al., published the first full QCD lattice simulation of the direct insertion calculation with high statistics. Their result, along with calculations from other analyses is shown in Table 2.5. 

Type of Calculation	μ_s	Reference
Lattice QCD	-0.017(25)(07)	[Doi09]
Dispersion relation with Pole ansatz	-0.31(9)	[Jaf89]
Dispersion relation with Kaon Clouds	-(0.15→0.51)	[HRM99]
Quark Model	0.035	[GI97]
Chiral Quark-Soliton Model	0.08-0.13	[SKUG06]

Table 2.5: *Summary of theoretical predictions for $\mu_s s$.*

Bibliography

- [Ams08] C. et al. (Particle Data Group) Amsler. Review of particle physics. *Phys. Lett.*, B667:1, 2008.
- [BAB08] Arie Bodek, S. Avvakumov, R. Bradford, and Howard Scott Budd. Extraction of the Axial Nucleon Form Factor from Neutrino Experiments on Deuterium. *J. Phys. Conf. Ser.*, 110:082004, 2008.
- [Bec89] D. H. Beck. Strange-quark vector currents and parity-violating electron scattering from the nucleon and from nuclei. *Phys. Rev. D*, 39(11):3248–3256, Jun 1989.
- [Bei05] Elizabeth J. Beise. The axial form factor of the nucleon. *Eur. Phys. J.*, A24S2:43–46, 2005.
- [BH55] H.A. Bethe and F. De Hoffmann. *The Mesons and Fields*. Row, Peterson and Company., 1955.
- [BH01] D. H. Beck and B. R. Holstein. Nucleon structure and parity-violating electron scattering. 2001.
- [BM01] D. H. Beck and R. D. McKeown. Parity-violating electron scattering and nucleon structure. 2001.
- [BMT05] P. G. Blunden, W. Melnitchouk, and J. A. Tjon. Two-photon exchange in elastic electron nucleon scattering. *Phys. Rev.*, C72:034612, 2005.
- [BPS04] E. J. Beise, M. L. Pitt, and D. T. Spayde. The sample experiment and weak nucleon structure. 2004.
- [CFN93] Thomas D. Cohen, Hilmar Forkel, and Marina Nielsen. Just how strange? loops, poles and the strangeness radius of the nucleon. 1993.
- [DGH92] J. F. Donoghue, E. Golowich, and Barry R. Holstein. Dynamics of the standard model. *Camb. Monogr. Part. Phys. Nucl. Phys. Cosmol.*, 2:1–540, 1992.
- [Doi09] T. et al. Doi. Nucleon strangeness form factors from $N_f = 2 + 1$ clover fermion lattice QCD. 2009.
- [GI97] Paul Geiger and Nathan Isgur. Strange hadronic loops of the proton: A quark model calculation. *Phys. Rev.*, D55:299–310, 1997.
- [Got00] Y. et al. Goto. Polarized parton distribution functions in the nucleon. *Phys. Rev. D*, 62(3):034017, Jul 2000.

- [H76] G. et al. Höller. Analysis of electromagnetic nucleon form factors. *Nucl. Phys.*, B114, 1976.
- [HM84] Francis Halzen and Alan D. Martin. *The Quarks & Leptons: An Introductory Course in Modern Particle Physics*. John Wiley & Sons, Inc., 1984.
- [HPD92] E. Hadjimichael, G. I. Poulis, and T. W. Donnelly. Parity-violating asymmetry in quasielastic e-d scattering. *Phys. Rev. C*, 45(6):2666–2682, Jun 1992.
- [HRM99] H. W. Hammer and M. J. Ramsey-Musolf. K anti-K continuum and isoscalar nucleon form factors. *Phys. Rev.*, C60:045204, 1999.
- [Jaf89] R. L. Jaffe. Stranger Than Fiction: The Strangeness Radius and Magnetic Moment of the Nucleon. *Phys. Lett.*, B229:275, 1989.
- [KHP92] W. Koepf, E. M. Henley, and S. J. Pollock. Strangeness matrix elements in the nucleon. *Phys. Lett.*, B288:11–17, 1992.
- [KM88] David B. Kaplan and Aneesh Manohar. Strange Matrix Elements in the Proton from Neutral Current Experiments. *Nucl. Phys.*, B310:527, 1988.
- [LMRM07] Jianguai Liu, Robert D. McKeown, and Michael J. Ramsey-Musolf. Global Analysis of Nucleon Strange Form Factors at Low Q^2 . *Phys. Rev.*, C76:025202, 2007.
- [MB94] M. J. Musolf and M. Burkardt. Stranger still: Kaon loops and strange quark matrix elements of the nucleon. *Zeitschrift für Physik C*, 61:433, 1994.
- [McK89] R. D. McKeown. Sensitivity of Polarized Elastic electron Proton Scattering to the Anomalous Baryon Number Magnetic Moment. *Phys. Lett.*, B219:140–142, 1989.
- [Mil98] Gerald A. Miller. Nucleon charge symmetry breaking and parity violating electron-proton scattering. *Phys. Rev. C*, 57(3):1492–1505, Mar 1998.
- [MS84] W. J. Marciano and A. Sirlin. Some general properties of the $o(\alpha)$ corrections to parity violation in atoms. *Phys. Rev. D*, 29(1):75–88, Jan 1984.
- [Mus94] M. J. et al. Musolf. Intermediate-energy semileptonic probes of the hadronic neutral current. *Phys. Rept.*, 239:1–178, 1994.
- [RMI97] M. J. Ramsey-Musolf and Hiroshi Ito. Chiral symmetry and the nucleon’s vector strangeness form factors. *Phys. Rev. C*, 55(6):3066–3082, Jun 1997.

- [RS74] E. Reya and K. Schilcher. Neutral-current effects in elastic electron-nucleon scattering. *Phys. Rev. D*, 10(3):952–959, Aug 1974.
- [Sac62] R. G. Sachs. High-energy behavior of nucleon electromagnetic form factors. *Phys. Rev.*, 126(6):2256–2260, Jun 1962.
- [SKUG06] Antonio Silva, Hyun-Chul Kim, Diana Urbano, and Klaus Goeke. Parity-violating asymmetries in elastic e(pol.) p scattering in the chiral quark-soliton model: Comparison with A4, G0, HAPPEX and SAMPLE. *Phys. Rev.*, D74:054011, 2006.
- [TBM09] J. A. Tjon, P. G. Blunden, and W. Melnitchouk. Detailed analysis of two-boson exchange in parity-violating e-p scattering. *Physical Review C (Nuclear Physics)*, 79(5):055201, 2009.
- [ZPHRM00] Shi-Lin Zhu, S. J. Puglia, B. R. Holstein, and M. J. Ramsey-Musolf. Nucleon anapole moment and parity-violating ep scattering. *Phys. Rev. D*, 62(3):033008, Jul 2000.